

Impact of amiodarone and cisapride on simulated human ventricular electrophysiology and electrocardiograms

Mathias Wilhelms^{1*}, Christian Rombach¹, Eberhard P. Scholz², Olaf Dössel¹, and Gunnar Seemann¹

¹Institute of Biomedical Engineering, Karlsruhe Institute of Technology (KIT), Kaiserstr. 12, 76131 Karlsruhe, Germany; and ²Department of Internal Medicine III, University Hospital Heidelberg, 69120 Heidelberg, Germany

Aims

Amiodarone and cisapride are both known to prolong the QT interval, yet the two drugs have different effects on arrhythmia. Cisapride can cause torsades de pointes while amiodarone is found to be anti-arrhythmic. A computational model was used to investigate the action of these two drugs.

Methods and results

In a biophysically detailed model, the ion current conductivities affected by both drugs were reduced in order to simulate the pharmacological effects in healthy and ischaemic cells. Furthermore, restitution curves of the action potential duration (APD), effective refractory period, conduction velocity, wavelength, and the vulnerable window were determined in a one-dimensional (1D) tissue strand. Moreover, cardiac excitation propagation was computed in a 3D model of healthy ventricles. The corresponding body surface potentials were calculated and standard 12-lead electrocardiograms were derived. Both cisapride and amiodarone caused a prolongation of the QT interval and the refractory period. However, cisapride did not significantly alter the conduction-related properties, such as e.g. the wavelength or vulnerable window, whereas amiodarone had a larger impact on them. It slightly flattened the APD restitution slope and furthermore reduced the conduction velocity and wavelength.

Conclusion

Both drugs show similar prolongation of the QT interval, although they present different electrophysiological properties in the single-cell as well as in tissue simulations of cardiac excitation propagation. These computer simulations help to better understand the underlying mechanisms responsible for the initiation or termination of arrhythmias caused by amiodarone and cisapride.

Keywords

Mathematical model • Cardiac ischaemia • Drugs • Body surface potentials

Introduction

Development of new pharmacological agents is a time-consuming and expensive process,¹ during which adverse side effects should be identified in an early stage. For the assessment of the cardiac toxicity of drugs, i.e. if a drug induces arrhythmias, reliable biomarkers have to be identified. One of them used in the process of drug development is the prolongation of the QT interval of the electrocardiogram (ECG). Both drugs investigated in this work, amiodarone and cisapride, prolong the QT interval.^{2,3} On the one hand, amiodarone is a class III anti-arrhythmic agent. This multi-channel blocker affecting inward sodium and calcium channels as well as repolarizing outward potassium channels⁴ is used for the treatment of atrial or ventricular tachycardia. Cisapride, on the other

hand, is a gastrointestinal prokinetic agent, whose main action is to inhibit the rapid delayed rectifier potassium current I_{Kr} .⁵ Therefore, it led to the occurrence of torsades de pointes and was consequently withdrawn from market.³

In recent years, *in silico* modelling of cardiac drug effects started developing, e.g. for the investigation of adverse side effects or the impact on arrhythmias.^{6–10} For this purpose, drug effects were integrated into mathematical models of cardiac electrophysiology. The integration can be achieved by e.g. adaptation of ion channel conductivities of the model to the dose-dependent inhibition of these currents. The dose-dependent inhibition is quantitatively described by the IC_{50} and nH value, which define the half-maximal inhibitory concentration and the slope of the Hill curve. Then, the effects, which are measured at the ion channel level by e.g. voltage

* Corresponding author. Tel: +49 721 608 42790; fax: +49 721 608 42789, Email: publications@ibt.kit.edu

Published on behalf of the European Society of Cardiology. All rights reserved. © The Author 2012. For permissions please email: journals.permissions@oup.com.

clamp protocols, can be simulated at the cell, tissue, or even organ level. In that way, the impact of the drug on the body surface potentials and the ECG can be computed.¹¹

Amiodarone is recommended as a treatment option following electrical cardioversion in case of occurrence of arrhythmias in the guidelines for the management of myocardial infarction.¹² Therefore, in this work, the effects of amiodarone and cisapride were investigated in ischaemic tissue as well. During the first minutes of cardiac ischaemia, different electrophysiological changes occur in the affected myocardium due to the occlusion of a coronary artery: hypoxia, acidosis, and extracellular hyperkalaemia. These biochemical alterations also cause an adaptation of electrophysiological properties of the tissue: the action potential (AP) amplitude and the action potential duration (APD) decrease, whereas the resting membrane voltage and the refractory period (prolongation of post-repolarization refractoriness) increase.¹³ Furthermore, these changes often lead to ventricular tachycardia or fibrillation during the first 2–10 min of ischaemia, which can be subdivided into stage 1 at around 5 min and stage 2 at around 10 min.

In the present computational study, the electrophysiological properties as e.g. effective refractory period (ERP), conduction velocity (CV), wavelength (WL), or vulnerable window (VW) of healthy and ischaemic ventricular tissue were studied under the influence of amiodarone and cisapride. Furthermore, the impact of both drugs on the body surface ECG and the QT interval was investigated. In this way, amiodarone and cisapride, which show similar ECG changes, but opposite effects on the heart rhythm in clinical practice, were analysed on different simulation scales to determine the origin of their contrary properties.

Methods

Modelling ventricular electrophysiology

In this work, a modified version of the model published by ten Tusscher *et al.*¹⁴ in 2006 was used. It offers a detailed description of the ventricular electrophysiology of endocardial, M, and epicardial cells. The main effects of acute cardiac ischaemia, hypoxia, acidosis, and extracellular hyperkalaemia were incorporated into the model to account for the electrophysiological changes at stage 1 as shown in ref.¹⁵ In this way, transmurally varying ischaemia effects were modelled, with the strongest impact on epicardial cells due to the higher sensitivity of adenosine triphosphate (ATP)-regulated potassium channels $I_{K,ATP}$.

In order to account for the impact of cisapride and amiodarone on cardiac ion currents, the respective reduction of ionic currents due to the drugs was determined using IC_{50} and nH values reported in the literature (Table 1). If only a dose-dependent reduction was published, a Hill curve was fitted to the given data. The reduction of $hERG/I_{Kr}$, which is the only current affected by therapeutic concentrations of cisapride,¹⁶ was described in ref.¹⁷ In case of amiodarone, the IC_{50} and nH values found in the literature varied by one order of magnitude for two ionic channels. Therefore, two setups with different values for $hERG/I_{Kr}$ and the L-type calcium current I_{CaL} were created (compare Table 1). Setup 1 (S1) used the values of Wu *et al.*¹⁸ for $hERG$ and of Nishimura *et al.*¹⁹ for I_{CaL} , whereas Setup 2 (S2) relied on the data of Ridley *et al.*²⁰ and Varro *et al.*²¹ respectively. The values for the sodium current I_{Na} ,²² the sodium potassium pump I_{NaK} ,²³ the sodium calcium exchanger I_{NaCa} ²⁴ and the slow delayed rectifier potassium current I_{Ks} ²⁵ were the same in both setups. To determine the relative inhibition of the ion channel conductivities from these data, two concentrations in the therapeutic range of the drugs were chosen. For cisapride, the low concentration was 150 nM and the high dose was 300 nM. However, more than 95% of cisapride is bound to plasma proteins.¹⁷ Therefore, the effective concentration used for the calculation of the inhibition of I_{Kr} was corrected by this factor. For amiodarone, the range of therapeutic concentrations is between 1 and 3 μM ,⁴ giving the low and high concentrations used for the simulations. The resulting ion channel conductivity reductions relative to their original values are given in Table 2.

Single-cell investigations

The healthy ventricular cells were paced for 40 s with a basic cycle length (BCL) of 1 s, whereas the ischaemic cells were paced for 360 s with a BCL of 1 s until they reached stage 1 (5 min). The onset of ischaemia effects was at 60 s. After the initial pacing, the resulting amplitude and APD_{90} of the healthy and ischaemic endocardial, M, and epicardial cells with and without the influence of drugs were measured.

One-dimensional tissue strand

A homogeneous one-dimensional (1D) tissue strand and the monodomain model were used for the computation of the steady state restitution curves of the ERP, the slope of the APD_{90} ($\delta APD_{90}/\delta DI$), the CV, the WL, and the VW. The electrophysiological model was initialized in a single-cell environment first, so that it could adapt to the different BCLs, the different ischaemia stages and the drug effects. As in the single-cell simulations, the healthy cells were paced for 40 s and the ischaemic ones for 360 s. Then, the 1D tissue strand was stimulated five times and the last beat was investigated only, if all previous stimulations could initiate an AP. The stimulus was applied to one end of the

Table 1 Inhibition of cardiac ion currents

Drug	Cisapride	Amiodarone		I_{Na}	I_{NaK}	I_{CaL} S1/ I_{CaL} S2	I_{NaCa}	I_{Ks}
		I_{Kr}	I_{Kr} S1/ I_{Kr} S2					
IC_{50} (μM)	0.023	0.8/0.07	1.4	15.6	5.8/0.55	3.3	3.84	
nH	0.8	1.3/1.1	1.0	1.0	1.0/0.26	1.0	0.63	
Source	17	18/20	22	23	19/21	24	25	

Data used in this work showing inhibition of ion currents caused by cisapride and amiodarone. Two values each for I_{Kr} and I_{CaL} in the case of amiodarone are used for two different setups. First value is used for Setup 1 (S1) and second one for Setup 2 (S2).

Table 2 Reduction of ion channel conductivities

Conductivity	Cisapride		Amiodarone Setup 1 (S1)		Amiodarone Setup 2 (S2)	
	Low	High	Low	High	Low	High
g_{Kr}	71.44	58.97	42.80	15.21	5.09	1.58
g_{Na}	100	100	58.33	31.82	58.33	31.82
P_{NaK}	100	100	93.98	83.87	93.98	83.87
g_{CaL}	100	100	85.29	65.91	46.12	39.15
k_{NaCa}	100	100	76.74	52.38	76.74	52.38
g_{Ks}	100	100	80.20	69.50	80.20	69.50

Reduction of ion channel conductivities (% of original value) due to cisapride and amiodarone. Definition of concentrations: cisapride low (150 nM) and high (300 nM), amiodarone low (1 μ M) and high (3 μ M).

fibre. The APD_{90} was measured at the centre of the second half of the strand to determine the diastolic interval ($DI = BCL - APD_{90}$). The CV was calculated by measurement of the activation times at two distant points, one at the centre of the first half and one at the centre of the second half of the fibre. Additional premature stimuli placed at the same stimulation site as before were used for the determination of the ERP. The WL was calculated as the product of CV and ERP. This was done for BCLs between 0.3 and 1.3 s in healthy and 0.4 and 1.7 s in ischaemic tissue to determine restitution properties. In this work, the VW was defined as the interval during which a unidirectional block could be initiated. This critical time span was determined by stimulating prematurely at the centre of the strand and a successful detection of an AP in the centre of the first half of the strand and no AP in the centre of the second half of the fibre.

Three-dimensional ventricular model

For the simulation of cardiac excitation propagation in healthy ventricles under the influence of drugs, a 3D voxel model derived from magnetic resonance (MR) images of a healthy volunteer and the monodomain model were used. The cardiac fibre orientation was generated using a rule-based method relying on the findings of Streeter *et al.*²⁶ The His-Purkinje conduction system was mimicked by an endocardial stimulation profile as used in.²⁷ For the consideration of different heterogeneities, the ventricular wall was divided into each 40% endocardial and midmyocardial tissue, and 20% epicardial tissue. In this way, transmurally varying parameters of the transient outward potassium current I_{to} and the slow delayed potassium current I_{Ks} could be used as suggested in the original model.¹⁴ Additionally, the conductivity g_{Ks} was modelled heterogeneously from apex to base, with the apical value being twice as big as the original value at the base.²⁷ The heterogeneous electrophysiological models were first initialized for 40 s in a single-cell environment with a BCL of 1 s. Then, the excitation propagation with and without the influence of drugs was simulated in the 3D ventricular model. Since cardiac ischaemia has a significant impact on ventricular excitation propagation and also the body surface ECG,¹⁵ the impact of drugs on the ECG was simulated in healthy ventricles.

Forward calculation of body surface potentials

A high-resolution torso model is needed for the forward calculation based on transmembrane voltage distributions computed with the monodomain equations.²⁸ In this work, the tetrahedral thorax model

was also derived from MR images of the same healthy volunteer.²⁷ The transmembrane voltage distributions in the 3D ventricular voxel model were interpolated on the tetrahedral thorax mesh. Afterwards, the elliptical part of the bidomain model was used for the computation of the body surface potential maps (BSPMs) considering inhomogeneous tissue conductivities.²⁹ Standard 12-lead ECGs were then derived from the BSPMs. In this work, the QT interval was determined by definition of the onset of the QRS complex (Q_{onset}) and detection of the end of the T-wave (T_{end}). The endocardial stimulation profile used for the simulation of cardiac excitation propagation defined Q_{onset} ($t = 0$ ms). The time, at which the ECG signal fell below a threshold ($V_{thresh} = 0.01$ mV) was defined as T_{end} , since there was no measurement noise, no baseline wander, and the baseline was nearly zero.

Numerical methods

For the computation of the ventricular electrophysiology, the Rush-Larsen scheme was used for the gating variables and the forward Euler scheme for the remaining ODEs of the model of ten Tusscher *et al.*¹⁴ A time increment of 20 μ s was sufficient for the single cell as well as the tissue simulations. Tissue simulations were computed by the modular and parallel excitation propagation solver acCELLerate.³⁰ The 1D tissue strand used for the calculation of the ERP, CV, and WL restitution consisted of 200 voxel and that for the calculation of the VW restitution of 400 voxel. The cubic voxel size was 0.2 mm in the 1D tissue strand and the isotropic intracellular conductivity was set to 0.19 S/m to obtain a CV of around 900 mm/s at a BCL of 1 s in the control case. Here, the finite difference method was used. The 3D ventricular model had a cubic voxel resolution of 0.4 mm and the monodomain conductivity, which varied transmurally, was on average 0.26 S/m with an anisotropy factor of 2.6 as in ref.²⁹ The finite-element method was used for the computation of the excitation propagation as well as for the forward calculation of BSPMs for every 1 ms on the high-resolution (about 0.75 million nodes) tetrahedral thorax mesh.

Results

Single-cell simulations

At first, the impact of cisapride and amiodarone on isolated healthy and ischaemic ventricular cells was investigated. Since ischaemia

effects were strongest in epicardial cells due to the higher sensitivity of $I_{K,ATP}$, the resulting APs of this cell type are shown in *Figure 1*. In endocardial and M cells, similar but less pronounced ischaemia effects could be observed. Effects of the investigated drugs on electrophysiological properties, such as the APD_{90} , were similar as in epicardial cells. The AP parameters of the different epicardial cells are given in *Table 3*. Compared with healthy ones, ischaemic cells showed a decreased amplitude and APD_{90} , whereas the resting membrane voltage $V_{m,rest}$ was elevated. Cisapride did not significantly alter the amplitude and $V_{m,rest}$. However, APD_{90} was prolonged with increasing drug concentration by between 3.6 and 5.3% in healthy and 5.0–7.3% in ischaemic cells. In the case of amiodarone, the amplitude was lowered by between 6.3 and 14.5% in healthy and 7.7–15.9% in ischaemic cells. Regarding the amplitude, the difference between S1 and S2 could be neglected. The APD_{90} of healthy epicardial cells was prolonged by 12–17.9% with increasing concentration of amiodarone S1 and by 6.1–9.9% with increasing concentration of amiodarone S2. During stage 1 ischaemia, APD_{90} was slightly prolonged by 1.28% using low concentration S1, whereas the high concentration S1 shortened it by 8.2%. Amiodarone S2 caused an APD_{90} reduction by 21.3–47.5%. Furthermore,

amiodarone caused a slight elevation of $V_{m,rest}$ in healthy and ischaemic cells.

Tissue restitution properties

In the 1D tissue strand, the ERP, APD_{90} slope, CV, and WL restitution curves were determined. As in the single-cell simulations, ischaemia effects were strongest in epicardial tissue and the impact of drugs on endocardial and midmyocardial tissue was similar. Therefore, the resulting curves of epicardial tissue are shown in *Figure 2*. Cardiac ischaemia led to an increase of the ERP and to a decrease of the CV, the WL, and the slope of the APD_{90} restitution curve. Furthermore, high concentration of amiodarone prevented excitation propagation in ischaemic epicardial tissue. Therefore, the corresponding restitution properties are not listed.

Cisapride increased the ERP moderately, whereas amiodarone showed a stronger prolongation in healthy tissue. In ischaemic tissue, cisapride caused a similar ERP as the control case and amiodarone prolonged the ERP by around 150 ms. The slope of the APD_{90} restitution increased towards shorter DIs in healthy tissue. Cisapride and the high concentration of amiodarone S1 showed a similar slope as the control tissue, whereas amiodarone S2 and the low concentration of S2 decreased the slope towards

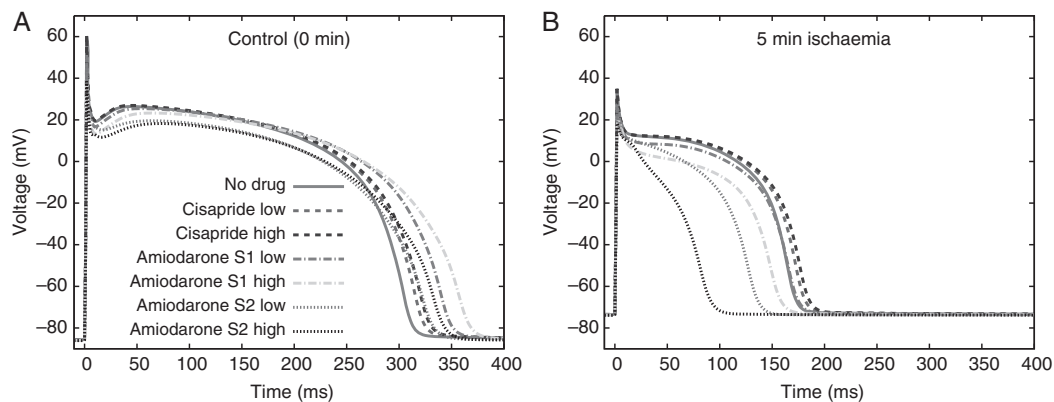


Figure 1 Action potentials of epicardial healthy control cells (A) and cells after 5 min of ischaemia (B). Drug-related changes of ion channels due to cisapride and amiodarone according to *Table 2*.

Table 3 Resulting action potential parameters

	0 min ischaemia (control)			5 min ischaemia (stage 1)		
	Amplitude (mV)	APD_{90} (ms)	$V_{m,rest}$ (mV)	Amplitude (mV)	APD_{90} (ms)	$V_{m,rest}$ (mV)
No drug	145.89	307.26	-85.62	108.45	169.75	-73.51
Cisa low	146.05	318.37	-85.61	108.38	178.17	-73.49
Cisa high	146.11	323.59	-85.60	108.36	182.08	-73.48
Amio S1 low	136.69	344.04	-85.73	99.30	171.92	-73.59
Amio S1 high	124.78	362.14	-85.91	92.96	155.78	-73.71
Amio S2 low	136.97	326.15	-86.00	100.08	133.64	-73.84
Amio S2 high	124.63	337.53	-86.09	91.26	89.14	-73.91

Changes of healthy and ischaemic single-cell epicardial AP parameters (amplitude, APD_{90} , $V_{m,rest}$) with and without the influence of cisapride and amiodarone.

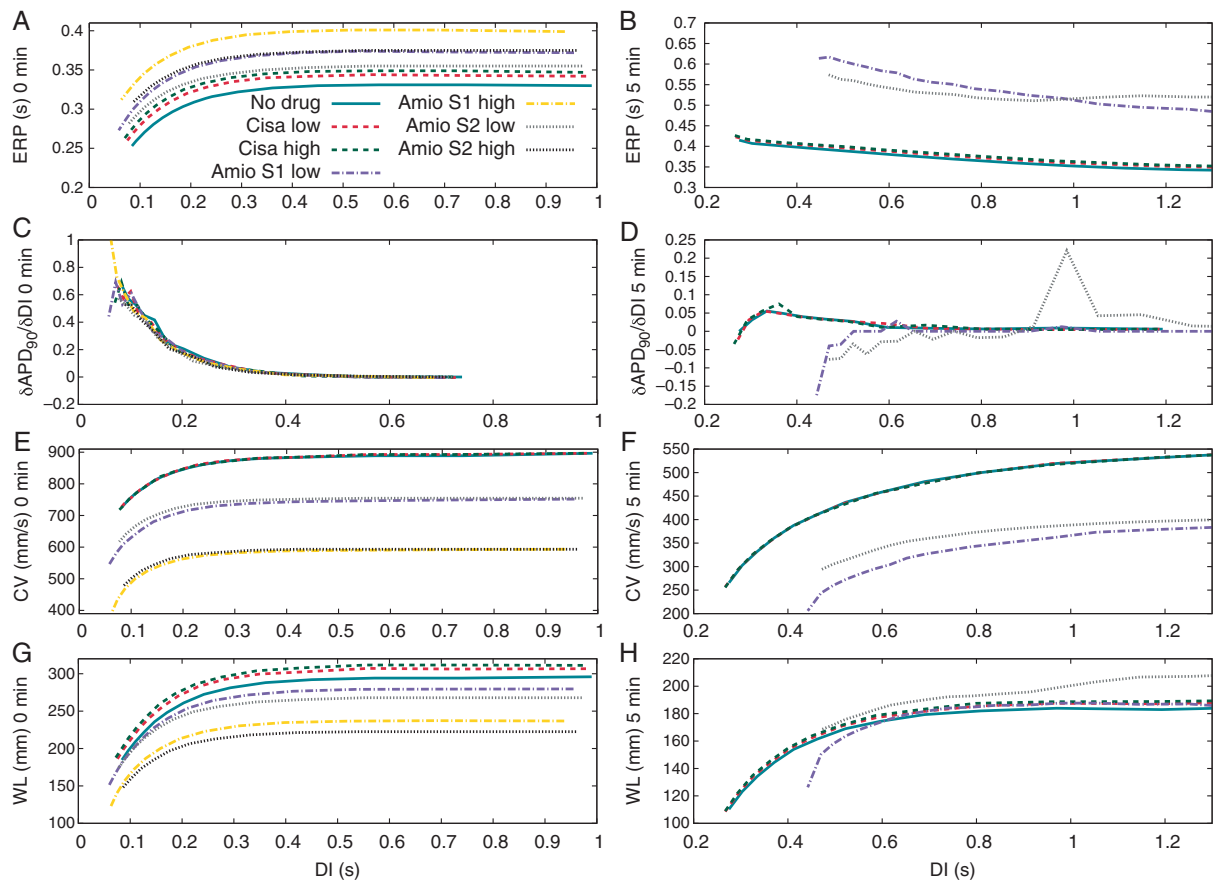


Figure 2 Restitution curves of healthy (left) and ischaemic (right) epicardial tissue. (A and B) Effective refractory period restitution, (C and D) slope of APD_{90} restitution, (E and F) conduction velocity restitution, and (G and H) wavelength restitution.

short DIs. During ischaemia, the control case and cisapride had the same slope of the APD_{90} restitution curve with values around 0, whereas amiodarone presented a negative slope towards short DIs. The CV was not affected by cisapride, whereas the low concentration of amiodarone slowed it by approximately 150 mm/s (-16%) and the high concentration by around 300 mm/s (-33%). Cisapride slightly increased the WL, whereas amiodarone shortened the WL in healthy tissue. During ischaemia, amiodarone prolonged the WL, although S1 decreased it at short DIs.

The VW was nearly constant at all DIs. Only at the shortest DI analysed, the VW was slightly higher (not shown). It was 0.3 ms at a BCL of 1 s in healthy control tissue. Cisapride and the low concentration of amiodarone S2 caused the same VW. Low concentration of amiodarone S1 led to a VW of 0.4 ms, whereas the high concentrations showed a longer VW of 0.5 ms (S2) and 0.6 ms (S1). During ischaemia, the VW was much longer with 12 ms in the control and cisapride cases, 17 ms in the case of amiodarone S1, and 33 ms in the case of amiodarone S2.

Ventricular excitation propagation and electrocardiograms

The cardiac excitation propagation was simulated using the 3D model of healthy ventricles. Compared with the control case,

only the repolarization phase was affected by cisapride, which delayed the complete repolarization of the ventricles. In contrast to that, amiodarone also changed the depolarization phase of the ventricles. The slowed conduction velocity delayed the complete activation of the ventricles. Furthermore, the maximum amplitude was also lowered and the repolarization was finished significantly later.

These changes of the excitation propagation pattern were also reflected in the BSPMs and the derived ECGs. Highest signal amplitudes and also most prominent changes could be observed in lead V_4 , which is shown in Figure 3. Cisapride did not change the QRS complex; however, the T-wave started and ended later. T_{end} was delayed by between 17 and 26 ms with increasing drug concentration. Low concentrations of amiodarone slightly prolonged the QRS complex, whereas high concentrations even delayed it and altered its amplitude. As cisapride, amiodarone S1 delayed the onset and additionally broadened the T-wave. Consequently, T_{end} was detected 47 ms (low concentration) and 75 ms (high concentration) later. Low concentration of amiodarone S2 also broadened the T-wave. Therefore, it started earlier and ended 39 ms later than the control case. High concentration of amiodarone S2 caused a later onset and a lower amplitude of the T-wave but almost the same T_{end} as the low concentration of S1.

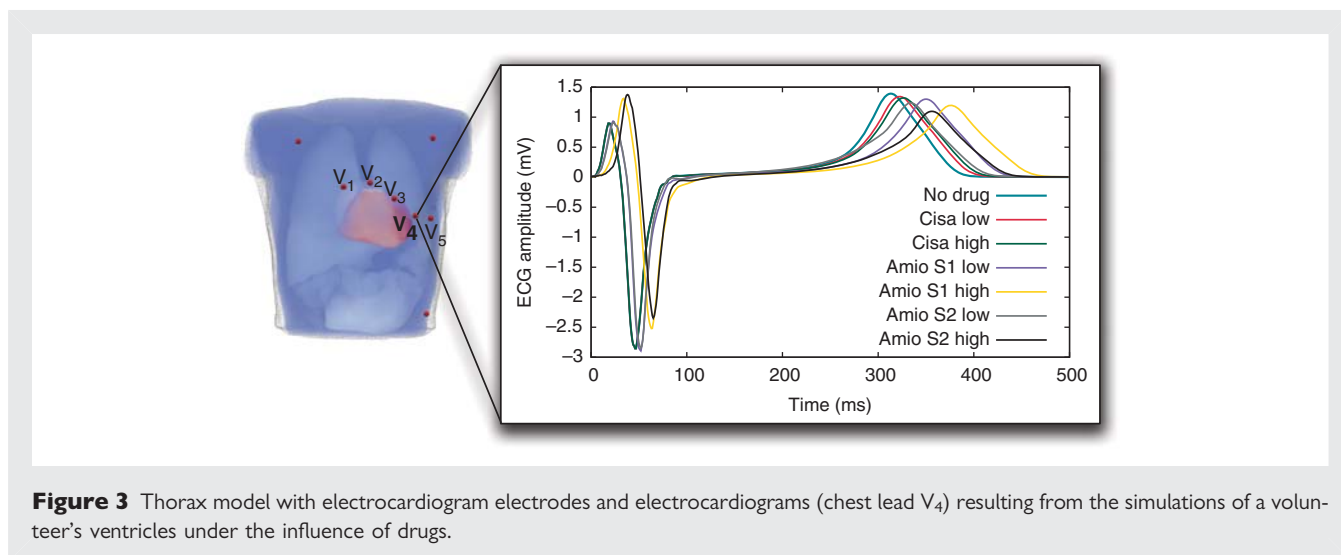


Figure 3 Thorax model with electrocardiogram electrodes and electrocardiograms (chest lead V₄) resulting from the simulations of a volunteer's ventricles under the influence of drugs.

Discussion

Drug-induced arrhythmias such as torsades de pointes are a major problem for drug development. Therefore, certain biomarkers indicating this cardiotoxicity have to be investigated thoroughly.³¹ One of these biomarkers used for the detection of pro-arrhythmic drugs is the prolongation of the QT interval. However, also some anti-arrhythmic drugs cause a prolongation of the QT interval, indicating that this biomarker alone is not necessarily useful for the identification of drug-induced arrhythmias.³²

In this work, the impact of cisapride and amiodarone on simulated cardiac electrophysiology and ECGs were investigated. For this purpose, different dose-dependent inhibitory effects of both drugs were integrated into a model of healthy and ischaemic ventricular myocytes causing various changes of AP morphology and duration. The experimental data of the pharmacological inhibition of ionic currents used in this work varied markedly depending on the species, the cell type or the temperature used during the measurements. Therefore, two setups S1 and S2 with different values for I_{Kr} and I_{CaL} were created for the simulation of the effects of amiodarone on cardiac electrophysiology. Due to this, the results of both setups differed markedly. APD_{90} was slightly increased by amiodarone S2 and cisapride, whereas it was significantly prolonged by amiodarone S1 in healthy cells. The experimentally determined APD_{90} after acute administration of amiodarone is conflicting in the literature as well.⁴ Therefore, a direct comparison of simulated and experimental values is complicated. Further simulations aimed at investigating restitution properties in a 1D tissue strand. Both drugs increased the ERP. However, the main effect that could be observed in simulations of amiodarone was the CV reduction due to inhibition of I_{Na} and therefore also a shortening of the WL. Finally, the effects of cisapride and amiodarone were investigated in a 3D model of healthy ventricles and the derived ECG. Both drugs caused a later end of the T-wave and therefore also a prolongation of the QT interval.

The effects of a drug on the body surface ECG were also investigated in.¹¹ Therefore, dofetilide, which is another class III

anti-arrhythmic agent, was analysed in a computational study. However, the ventricles were stimulated apically resulting in a broad QRS complex, whereas an endocardial stimulation profile mimicking the His-Purkinje system was used in the present work. In ref.,⁷ D-sotalol and amiodarone were analysed in a 3D canine ventricular wedge with transmurally varying drug effects, which led to reduced transmural APD dispersion and therefore to reduced vulnerability in case of amiodarone. However, only changes of I_{NaL} , I_{CaL} , and I_{Ks} were considered for the simulation of effects of amiodarone and no body surface ECG was computed. Other modelling studies investigating the effects of drugs on cardiac electrophysiology can be found in, for example, refs.^{6,8,10}.

The experimental data used for the inhibition of I_{Na} probably overestimated the effects on this current, since a significant decrease of the CV or the broadening of the QRS complex is only reported at high pacing rates³³ and not at a BCL of 1 s. Due to this, the resulting WL and VW, which strongly depend on the CV, are mainly influenced by the reduced sodium channel conductivity. Both values would indicate a higher probability for the occurrence of arrhythmias. Repolarizing currents on the other hand determine the slope of the APD_{90} restitution and the ERP as well. As reported in ref.,³⁴ a flattening of APD restitution curve could be involved in the anti-arrhythmic action of amiodarone.

In this work, the definition of Q_{onset} , which marks the beginning of early ventricular depolarization, was based on the endocardial stimulation profile. It was equal for all ventricular simulations starting at $t = 0$ ms. Furthermore, a threshold voltage defined T_{end} . This criterion was chosen, since the simulated ECG signals showed a nearly zero baseline, no measurement noise and no baseline wander.

The present findings show the effects of amiodarone and cisapride in multi-scale simulations of cardiac electrophysiology. Both drugs caused a prolongation of the QT interval in the body surface ECG. However, electrophysiological properties, such as APD, CV, WL, or VW varied strongly between both drugs. Therefore, assessment of drug cardiotoxicity based on QT prolongation alone is not recommendable. Other biomarkers, which are more

closely related to the underlying mechanisms responsible for drug-induced arrhythmias, should be identified.

For future work in this field, integration of measurement data for the different ion channels of one species obtained at body temperature could provide a better insight into the mechanisms of action of drugs. Furthermore, transmural heterogeneity of drug effects could be included, if the experimental data are available. Drug-induced changes of the ion channel biophysics could also be considered by adapting the electrophysiological model to voltage clamp measurement data of the affected channels. Additionally, state- and frequency-dependent changes due to the drugs should be considered in future.

Conflict of interest: none declared.

Funding

This work was supported by the German Research Foundation (grant number DFG SE 1758/3-1).

References

- Morgan S, Grootendorst P, Lexchin J, Cunningham C, Greyson D. The cost of drug development: a systematic review. *Health Policy* 2011;**100**:4–17.
- Cubeddu LX. QT prolongation and fatal arrhythmias: a review of clinical implications and effects of drugs. *Am J Ther* 2003;**10**:452–7.
- Wysowski DK, Corken A, Gallo-Torres H, Talarico L, Rodriguez EM. Postmarketing reports of QT prolongation and ventricular arrhythmia in association with cisapride and Food and Drug Administration regulatory actions. *Am J Gastroenterol* 2001;**96**:1698–703.
- Kodama I, Kamiya K, Toyama J. Amiodarone: ionic and cellular mechanisms of action of the most promising class III agent. *Am J Cardiol* 1999;**84**:20r–8r.
- Drolet B, Khalifa M, Daleau P, Hamelin BA, Turgeon J. Block of the rapid component of the delayed rectifier potassium current by the prokinetic agent cisapride underlies drug-related lengthening of the QT interval. *Circulation* 1998;**97**:204–210.
- Tsujimae K, Suzuki S, Murakami S, Kurachi Y. Frequency-dependent effects of various IKr blockers on cardiac action potential duration in a human atrial model. *Am J Physiol Heart Circ Physiol* 2007;**293**:H660–9.
- Benson AP, Aslanidi OV, Zhang H, Holden AV. The canine virtual ventricular wall: a platform for dissecting pharmacological effects on propagation and arrhythmogenesis. *Prog Biophys Mol Biol* 2008;**96**:187–208.
- Rodriguez B, Burrage K, Gavaghan D, Grau V, Kohl P, Noble D. The systems biology approach to drug development: application to toxicity assessment of cardiac drugs. *Clin Pharmacol Ther* 2010;**88**:130–4.
- Aslanidi OV, Al-Owais M, Benson AP, Colman M, Garratt CJ, Gilbert SH et al. Virtual tissue engineering of the human atrium: Modelling pharmacological actions on atrial arrhythmogenesis. *Eur J Pharm Sci* 2012;**46**:209–21.
- Saiz J, Gomis-Tena J, Monserrat M, Ferrero J, Cardona K, Chorro J. Effects of the antiarrhythmic drug dofetilide on transmural dispersion of repolarization in ventricle: a computer modeling study. *IEEE Trans Biomed Eng* 2011;**58**:43–53.
- Zenzemi N, Bernabeu M, Saiz J, Rodriguez B. Simulating drug-induced effects on the heart: from ion channel to body surface electrocardiogram. In: Metaxas D, Axel L, eds. *FIMH 2011, LNCS*, vol. 6666. Springer Berlin, p259–66.
- Van de Werf F, Bax J, Betriu A, Blomstrom-Lundqvist C, Crea F, Falk V et al. Management of acute myocardial infarction in patients presenting with persistent ST-segment elevation: the task force on the management of ST-segment elevation acute myocardial infarction of the European Society of Cardiology 2008.
- Carmeliet E. Cardiac ionic currents and acute ischemia: from channels to arrhythmias. *Physiol Rev* 1999;**79**:917–1017.
- ten Tusscher K, Panfilov A. Alternans and spiral breakup in a human ventricular tissue model. *Am J Physiol Heart Circ Physiol* 2006;**291**:H1088–100.
- Wilhelms M, Dössel O, Seemann G. In silico investigation of electrically silent acute cardiac ischemia in the human ventricles. *IEEE Trans Biomed Eng* 2011;**58**:2961–4.
- Chiang C-E, Wang T-M, Luk H-N. Inhibition of L-type Ca(2+) current in guinea pig ventricular myocytes by cisapride. *J Biomed Sci* 2004;**11**:303–14.
- Walker BD, Singleton CB, Bursill JA, Wyse KR, Valenzuela SM, Qiu MR et al. Inhibition of the human ether-a-go-go-related gene (hERG) potassium channel by cisapride: affinity for open and inactivated states. *B J Pharmacol* 1999;**128**:444–50.
- Wu L, Rajamani S, Shryock JC, Li H, Ruskin J, Antzelevitch C et al. Augmentation of late sodium current unmasks the proarrhythmic effects of amiodarone. *Cardiovasc Res* 2008;**77**:481–8.
- Nishimura M, Follmer CH, Singer DH. Amiodarone blocks calcium current in single guinea pig ventricular myocytes. *J Pharmacol Exp Ther* 1989;**251**:650–9.
- Ridley JM, Milnes JT, Witchel HJ, Hancox JC. High affinity hERG K(+) channel blockade by the antiarrhythmic agent dronedarone: resistance to mutations of the S6 residues Y652 and F656. *Biochem Biophys Res Commun* 2004;**325**:883–91.
- Varro A, Virag L, Papp JG. Comparison of the chronic and acute effects of amiodarone on the calcium and potassium currents in rabbit isolated cardiac myocytes. *Br J Pharmacol* 1996;**117**:1181–6.
- Follmer CH, Aomine M, Yeh JZ, Singer DH. Amiodarone-induced block of sodium current in isolated cardiac cells. *J Pharmacol Exp Ther* 1987;**243**:187–94.
- Gray DF, Mihailidou AS, Hansen PS, Buhagiar KA, Bewick NL, Rasmussen HH et al. Amiodarone inhibits the Na(+)-K+ pump in rabbit cardiac myocytes after acute and chronic treatment. *J Pharmacol Exp Ther* 1998;**284**:75–82.
- Watanabe Y, Kimura J. Inhibitory effect of amiodarone on Na(+)/Ca(2+) exchange current in guinea-pig cardiac myocytes. *B J Pharmacol* 2000;**131**:80–4.
- Zankov DP, Ding WG, Matsuura H, Horie M. Open-state unblock characterizes acute inhibition of I_{Ks} potassium current by amiodarone in guinea pig ventricular myocytes. *J Cardiovasc Electrophysiol* 2005;**16**:314–22.
- Streeter DD. Handbook of physiology. Section 2: The Cardiovascular System, vol. 1. In: *The Heart, chap. Gross morphology and fiber geometry of the heart*. Baltimore: Williams and Wilkins: American Physiology Society; 1979. p61–112.
- Keller DUJ, Weiss DL, Dössel O, Seemann G. Influence of IKs heterogeneities on the genesis of the T-wave: a computational evaluation. *IEEE Trans Biomed Eng* 2012;**59**:311–22.
- Potse M, Dubé B, Richter J, Vinet A, Gulrajani R. A comparison of monodomain and bidomain reaction-diffusion models for action potential propagation in the human heart. *IEEE Trans Biomed Eng* 2006;**53**:2425–35.
- Keller DUJ, Weber FM, Seemann G, Dössel O. Ranking the influence of tissue conductivities on forward-calculated ECGs. *IEEE Trans Biomed Eng* 2010;**57**:1568–76.
- Seemann G, Sachse FB, Karl M, Weiss DL, Heuveline V, Dössel O. Framework for modular, flexible and efficient solving the cardiac bidomain equation using PETSc. *Math Ind* 2010;**15**:363–9.
- Darpö B. Detection and reporting of drug-induced proarrhythmias: room for improvement. *Europace* 2007;**9**(Suppl. 4):iv23–36.
- Antzelevitch C. Ionic, molecular, and cellular bases of QT-interval prolongation and torsade de pointes. *Europace* 2007;**9**(Suppl. 4):iv4–15.
- Morady F, DiCarlo L, Krol R, Baerman J, de Buitelir M. Acute and chronic effects of amiodarone on ventricular refractoriness, intraventricular conduction and ventricular tachycardia induction. *J Am Coll Cardiol* 1986;**7**:148–57.
- Omichi C, Zhou S, Lee MH, Naik A, Chang CM, Garfinkel A et al. Effects of amiodarone on wave front dynamics during ventricular fibrillation in isolated swine right ventricle. *Am J Physiol Heart Circ Physiol* 2002;**282**:H1063–70.